RISC-Linz
Research Institute for Symbolic Computation
Johannes Kepler University
A-4040 Linz, Austria, Europe

Enclosing Robot Links By Superellipses and Superellipsoids.

Carl Van GEEM

(January 1996)

RISC-Linz Report Series No. 96-01

Editors: RISC-Linz Faculty
E.S. Blurock, B. Buchberger, G. Collins, H. Hong, T. Jebelean, F. Lichtenberger, H. Mayr, P. Paule, J. Pfalzgraf, H. Rolletschek, W. Schreiner, S. Stifter, F. Winkler.

Supported by:

Copyright notice: Permission to copy is granted provided the title page is also copied.

Enclosing Robot Links By Superellipses and Superellipsoids.

Carl Van Geem
RISC-Linz
Research Institute for Symbolic Computation
Joh. Kepler University
A-4040 Linz, Austria
Internet: Carl.Van.Geem@risc.uni-linz.ac.at

January 1996

Abstract

As a part of an approach for solving the robot motion planning problem for robot arms, we want to decide whether or not a link collides with an obstacle for a given range of values for (some of) the joint parameters. We want to use the so called Roider Method for fast collision checking, and want to model the link by enclosing it by a superellips (in 2 dimensional space) or by a superellipsoid (in 3 dimensional space).

We show in this paper that it is possible to model these swept areas using some elementary geometrical and trigonometrical tools. We describe for all swept volumes occuring for some robot arm topologies the extreme points needed for the enclosure of solids by a superellips or by a superellipsoid. We also compute the volume of the swept areas and of the enclosing superellips or superellipsoid. The rate between these volumes is a measure for the accuracy of the enclosure.

1 Introduction

Superellipses and superellipsoids are useful and extremely versatile primitives for constructive solid models. They have been studied thoroughly in the literature (see [Barr 81], [Zarrugh 85]). A particular application of these solids in collision detection in robot simulation systems is described in [Stifter 91], where the so called Roider Method for collision checking is used (see also [Stifter 88c]).

We want to construct a non-uniform grid over the Configuration Space of a robot arm, and therefore have to be able to decide whether or not in a given cell there is a configuration for which the robot arm collides with an obstacle. In order to do this collision check with the Roider Method for superellipses (in the 2 dimensional case) or superellipsoids (in the 3 dimensional case), we have to enclose the area swept by a link of the robot arm (when joints are moved over the intervals determining the given cell) by a superellips or superellipsoid. On the grid we put a potential field in order to solve the motion planning problem for a robot arm (for more details on our planning approach, see [Van Geem 94]).

In [Dittenberger 87], [Stifter 88c], and [Stifter 88b] the problem of enclosing cylinders, cones, etc. is discussed. In essence, given a particular object, one just takes a set of *extreme points* whose convex hull enclose the object, and then puts a superellipsoid around these points. The same approach can be used here, for the swept volumes in which we are interested.

We will describe in very precise way how to proceed for the swept volumes of some particular kind of robot topologies. Our main goal in doing so was to prove our feeling that it is possible to find good enclosing superellipses or superellipsoids using some easy geometrical and trigonometrical tools. We need particularly good enclosures for the application we have in mind, because too much area within the superellipses or superellipsoids will give rise to too many blocked cells in the grid over Configuration Space, and in concequence there would be cases in which we would not be able to find a path although it exists during motion planning. We do not feel satisfied with general approaches for modelling the swept volumes.

We will also compare the volume of the swept area with the volume of the enclosing superellips or superellipsoid. The rate between them is a measure for the accurateness of the enclosure.

In Section 2 we consider a robot arm with two links and two rotational joints in 2 dimensional space. We study the swept volume of the second link. In Section 3 we describe the extreme points for the enclosure of the swept volume of the second link of that robot topology. In Section 4 we consider a robot with a rotational joint at the base support, and then three more joints: a transdlational joint followed by a rotational joint and finally a translational joint. We also describe the extreme points fot this topology in Section 5. In Section 6 we compute the volumes of the enclosing superellipses, and the volumes of the swept areas for both the topologies considered in the previous sections. In Section 7 we consider the same topologies as before, but this time we model the links by rectangles instead of by line segments. We determine the extreme points and compute the volumes of the swept areas. In Section 8 we thicken the rectangular links so that they become cylinders. We then are in a three dimensional case, and thus have to enclose the swept area by a superellipsoid. The joints rotate as before in a plane. We again look for the extreme points and compute the volume of the swept area.

2 Shapes of the Swept Volume of a Second Link in 2D.

In the following we will use the notation as introduced in Figure 1. We write o for the point at the base support, the second joint is placed in point a and rotated over angle α to point d, the furthest point of the second link is positioned originally in point b, which is rotated over angle β to position c. Points b and c are rotated over angle α to points e and f respectively. We denote ζ for the angle between lines oa and ab, and ξ for the angle between lines oa and ac, so $\xi = \zeta + \beta$.

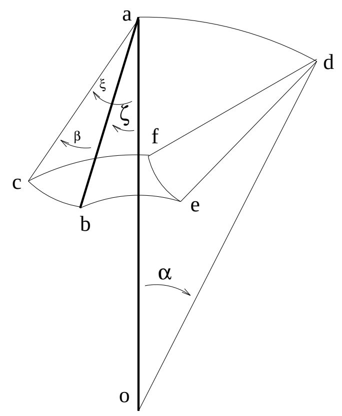

Figure 1: Notation.

There are four different cases for the shape of the swept volume. First of all notice the symmetry w.r.t. $\zeta + \xi = 2\pi$ (measuring the angles in the opposite direction, interchanging the roles of ζ and ξ). This reduces the cases by half. We further also assume that $\zeta - \xi < \frac{\pi}{2}$, which is a reasonable assumption for our application.

We can determine in which case we are in the following way, using the law of cosines for arbitrary triangles: Suppose ξ and ζ are both smaller than π. Then,

- For small values for angle ζ, point f is in the inside of the swept volume. If $\cos\xi \geq \frac{m}{2l}$ then we are in case 1,
- When ζ becomes sufficiently large, point a will lie in the interior of the swept volume and point f will lie on the boundary. If $\cos\xi < \frac{m}{2l}$ and $\cos\zeta \geq \frac{m}{2l}$, we are in case 2,
- When ζ is large, point a will lie on the boundary again and point e moves to the inside. If $\cos\zeta < \frac{m}{2l}$ we are in case 3,
- If $\cos\xi = \frac{m}{2l}$, then c and a sweep along the same line and thus we can proceed as in case 1,
- If $\cos\zeta = \frac{m}{2l}$, then a is on the same circle with center o and radius $\hat{n}$, where $\hat{n}$ is the distance between o and b. So this case is identical to case 2.

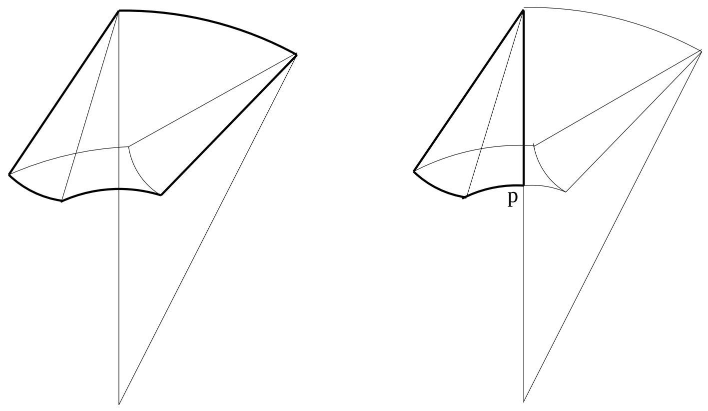

Figure 2: The first case: swept volume of second link, and point p.

If $\frac{\pi}{2} < \zeta < \pi < \xi$, we are in case 4.

We now prove the completeness of this case distinction by moving ξ and ζ along the unit circle and checking all possible cases. As in the previous we assume $\zeta - \xi < \frac{\pi}{2}$. In the first quadrant of the unit circle, for $0 < \zeta < \xi < \frac{\pi}{2}$, we see that $\cos\zeta > \cos\xi$. So, when $\cos\xi \geq \frac{m}{2l}$ we are in case 1. Since l and m will usually be of the same order of magnitude, $\frac{m}{2l}$ might be smaller than 1 rather often. For $\zeta, \xi < \frac{\pi}{2}$ it can happen that $\cos\xi < \frac{m}{2l}$, while $\cos\zeta \geq \frac{m}{2l}$. Then we are in case 2. When we increase the angles so that ξ ends up in the second quadrant of the unit circle, we get for $\xi > \frac{\pi}{2}$, $\cos\xi < 0 < \frac{m}{2l}$. Then we can have $\cos\zeta \geq \frac{m}{2l}$, corresponding to case 2. When instead $\cos\zeta < \frac{m}{2l}$, we are in case three. When both angles are in the second quadrant, that is $\frac{\pi}{2} < \xi < \zeta < \pi$, we naturally are in case 3. When $\frac{\pi}{2} < \xi < \pi$ and $\pi < \zeta < \frac{3\pi}{2}$, we end up with case 4.

3 Enclosing the Swept Volume of a Second Link in 2D.

We now come to the way how to enclose the shapes of the swept volume of the second link in the four essentially different cases:

case 1: First shape. Find point p, the intersection of line oa and circle segment bc (as in Figure 2; find point q, the intersection of the tangent in c to circle segment bc; find the superellips (as in [Stifter 91], [Stifter 88b]) enclosing the polygon $capbq$. The locally concave area and the rest of the swept volume are swept by the first link already.

For small values for α, the line oa does not intersect circle segment be. In that case we just take the polygon $bqcape$, where p now stands for the point of intersection of lines oa and de.

case 2: Second shape. Find point p, the intersetion of circle segment be and line oa. We denote s for the intersection of the tangent to curve segment cf in c and the tangent to curve segment cf in f. We denote t for the intersection of the tangent to curve segment bc in b and the tangent to curve segment bc in c. If the polygon d, p, b, t, c, s, f is convex, then we use it, else we use polygon d, e, b, t, c, s, f. This check has to be performed only on the area d, p, b. Find the enclosing superellips for the polygon. Remark: There is a nasty area created by the fact that c, f are not on circle segment ad but lie above it, i.e. an area not swept by the first link. Therefore we prefer modelling the whole area swept by the second link in this case.

Again for small values for angle α oa does not intersect circle segment be. We then just consider the polygon $debtcsf$.

case 3: Third shape. Find point p, the intersection of the tangent in b of circle segment bc and the tangent in c of circle segment bc; q the intersection of the tangent in c on circle segment cf and the tangent in f on circle segment cf. Enclose polygon a, d, f, q, c, p, b by a superellips.

case 4: Fourth shape. Find point s, the intersection of the circle segment bc and the line oa. Find t, the intersection of the circle segment ef and the line od. Denote p_1 for the intersection of the tangent to circle segment bs in b and the tangent to circle segment bs in s. Denote p_2 for the intersection of the tangent to circle segment st in s and the tangent to circle segment st in t. Denote p_3 for the intersection of the tangent to circle segment tf in t and the tangent to circle segment tf in f. Enclose the polygon $b, p_1, s, p_2, t, p_3, f, d, a$ by a superellips.

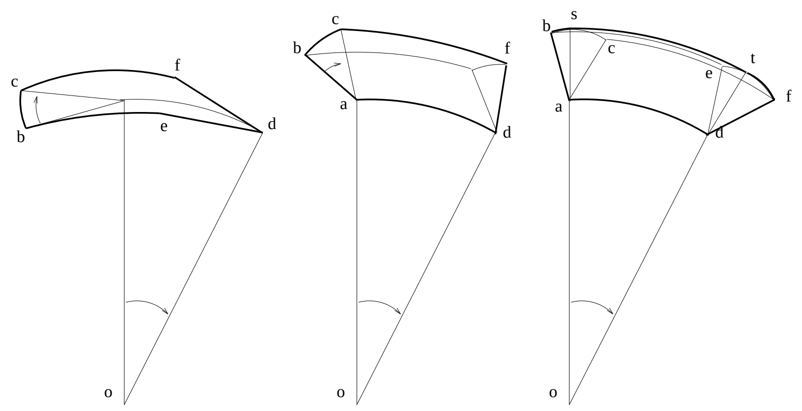

Figure 3: The cases 2, 3 and 4.

The vertices of the enclosing polygons constructed in the four cases are the extreme points for the algorithm in [Stifter 91]. However, also the direction of the axis of the cylinder from which the superellips is constructed, is free to choose in that algorithm. We suggest to chose for case 1 the line through the mass point of the extreme points and parallel to ab, and in the other cases the line through the mass point of the extreme points and parallel to ad.

4 Shapes of Swept Volume of a Third and Fourth Link in 2D.

Only small adaptations of the previous have to be made for extending it to two rotational joints alternated with two translational joints, in 2-dimensional Workspace.

We will denote the shortest possible distance between points o and a by l, between a and b by m. Any additional distance created by a move in the first translational joint will be denoted by l_e, and when created by a move in the second translational joint by m_e.

The first rotational joint is responsable for the creation of other shapes. Considering a coordinate frame in o with X-axis along the first link and Y-axis perpendicular to it. When $l_e = 0$, we have the shapes for the swept volume as in the previous sections. The extreme point g of that swept volume w.r.t. the Y-coordinate will give rise to a different shape in all four cases discussed in the previous sections. In the following we will denote $\tilde{x}$ for the point to which x is swept by a move over distance l_e in the first translational joint, $\bar{x}$ for the point to which x is swept by moving the first rotational joint over the total angle range considered. The notations are now like in Figure 4. We will denote x' for the point to which point x is swept by moving the second translational joint over a distance m_e.

Ignoring the first rotational joint for now, each point in the swept volume of the third link over the considered angle range for the second rotational joint will be swept over an interval of length l_e parallel to the first two links. This happens in each position of that swept volume, when it is swept over the considered angle range for the first rotational joint. Roughly, the resulting swept volume is thickened by l_e compared to the previous case. Starting from the four cases found in the previous sections, we come to the four cases as depictured in Figure 4, of which easily can be checked they are the only cases up to some symmetry considerations.

To conclude this section, we observe that the second translational joint does not induce any change to the shape of the swept volume. Indeed if we assume that the initial distance between a and b was m, we then computed the swept volume and then want to take into account a change in the distance between a and b by m_e, then we will end up with the swept volume as if we would have computed it with initial distance between a and b equal to $m + m_e$. So by this we are also done with the fourth link.

5 Enclosing the Swept Volume of a Third and Fourth Link in 2D.

For the third and fourth link, we have still four cases for the shapes, but the sets of extreme points (vertices of an enclosing polygon) are different. For the third link we get the following situation.

case 1: First Shape. Since $\xi, \zeta < \frac{\pi}{2}$, g has to be c. Take the polygon $b, q, c, \tilde{c}, \tilde{a}, p$, where q is the intersection of the tangent to bc in b and the tangent to bc in c.

For small values for α for which oa will not intersect circle segment be, we consider $b, c, \tilde{c}, q, \tilde{a}, p, e$, where now p stands for the intersection point of lines oa and de.

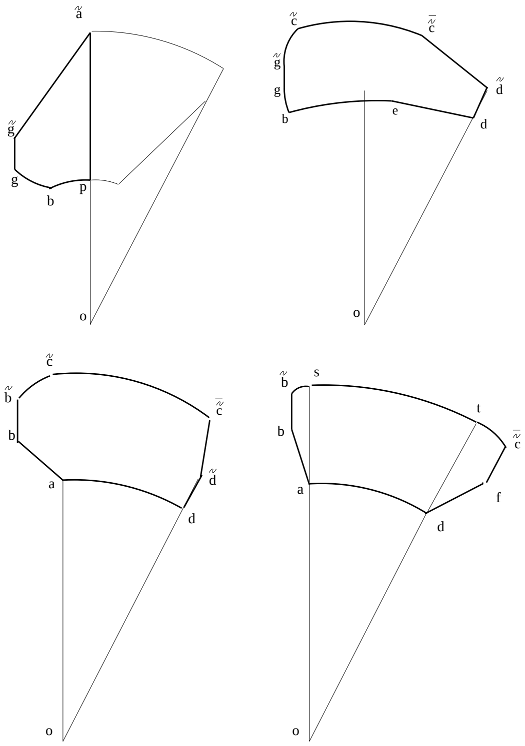

Figure 4: The four cases for third (and fourth) link.

case 2: Second Shape. Again, if b, p, d makes a convex area, we use polygon $d, p, b, g, \tilde{g}, \tilde{c}, \bar{\tilde{c}}, \tilde{d}$, else we use $d, e, b, g, \tilde{g}, \tilde{c}, \bar{\tilde{c}}, \tilde{d}$. Note that $\bar{\tilde{c}}$ can also be written as $\tilde{f}$.

Again for small values for α for which oa will not intersect circle segment be, we consider here the points $b, g, \tilde{g}, \tilde{c}, \bar{\tilde{c}}, \tilde{d}, d, e$.

case 3: Third Shape. Take the polygon $d, a, b, \tilde{b}, p, \tilde{c}, q, \bar{\tilde{c}}, f$, where p is the intersection of the tangent to $\tilde{b}\tilde{c}$ in $\tilde{b}$ and the tangent to $\tilde{b}\tilde{c}$ in $\tilde{c}$, and q the intersection of the tangent to $\tilde{c}\bar{\tilde{c}}$ in $\tilde{c}$ and the tangent to $\tilde{c}\bar{\tilde{c}}$ in $\bar{\tilde{c}}$. Note that g now coincides with b.

case 4: Fourth Shape. Take the polygon $d, a, b, \tilde{b}, s, t, \bar{\tilde{c}}, f$, where s is the intersection of $\tilde{b}\tilde{c}$ and oa, and t is the intersection of $\bar{\tilde{b}}\bar{\tilde{c}}$ and od. Note that g now coincides with b.

Considering the axis of the cylinder, we suggest to choose for case 1 the line through the mass point of the extreme points and parallel to ab, and in the other cases the line through the mass point of the extreme points and parallel to ad, as in the previous.

For the fourth link we replace x by x' in the previous, for $x \in \{b, c, e, f\}$.

6 Volume: Error Estimate.

In order to get an impression of the accuracy of the approximation of the swept volume of a link by the superellips we constructed in the previous sections, we can compute the volumes of both the swept volume of the link and of the superellips and compare them.

6.1 Volume of Superellips.

We will derive a formula for the volume of a superellips, in the way done in [Zarrugh 85] for superellipsoids. A superellips is determined by its center and three parameters A, B, and n. The superellips centered in the origin of a carthesian coordinate system is gien by the set

$$\{(A\cos^{1/n}\psi, B\sin^{1/n}\psi)\ ;\ \psi \in [0, 2\pi[, \}$$

for fixed A, B, n. This also corresponds to the equation $\left(\frac{x}{A}\right)^{2n} + \left(\frac{y}{B}\right)^{2n} = 1$.

Introducing the polar coordinates r, θ by

$$\begin{cases} \bar{x} = \frac{x}{A} = r\cos\theta, \\ \bar{y} = \frac{y}{B} = r\sin\theta, \end{cases}$$

we find the equation

$$(r\cos\theta)^{2n} + (r\sin\theta)^{2n} = 1,$$

from which we find for r:

$$r = (\cos^{2n}\theta + \sin^{2n}\theta)^{\frac{-1}{2n}}.$$

Taking slices of equal size for θ, the area of such a slice equals $\frac{r^2 d\theta}{2}$ and therefore the area of the superellips will be equal to

$$8\int_0^{\frac{\pi}{4}}((\cos^{2n}\theta + \sin^{2n}\theta)^{\frac{-1}{n}})d\theta.$$

For particular values of n a sufficiently good approximation of this integral is computed by the computer algebra system Maple. This result has to be multiplied still with A and B in order to get the volume of the superellips enclosing the swept volume.

In order to be able to make use of this formula we have to determine A, B and n for the superellipses constructed in the previous sections. If we allow a tolerance ϵ as in [Stifter 91], the algorithm there (simplified doing only the step for a superellips) will provide a value for A, B and n.

6.2 Volume of Swept Volume for Second Link in the 2 DOF Case.

We now come to the computation of the volume taken by the swept volume of the second link. In the following we will denote $Vol(SV_\delta([u, v]))$ for the volume taken by sweeping the interval $[u, v]$ over angle δ revolving around center u. Denoting D for the length of interval $[u, v]$, this area is equal to $\frac{\delta}{2}D^2$.

case 1: Here the volume is equal to $Vol(SV_\beta([a,b]))$ + ($Vol(\Delta a,b,o)$ - $Vol(SV_\gamma([o,b]))$), where $Vol(\Delta a,b,o)$ is the volume of the triangle with vertices a, b and o and γ the angle between lines oa and ob.

For small angles a slight adaptation has to be made to this computation. In this case we get the volume by $Vol(SV_\beta([ab])) + Vol(\Delta abo) - (Vol(SV_\alpha([ob])) + Vol(\Delta oep))$, where p now is the intersection of lines de and oa.

case 2: Let q be the intersection point of circle segment cf and line oa, p the intersection point of oa and circle segment be as in the previous. Then the volume is equal to ($Vol(SV_\alpha[oq])$ - $Vol(SV_\alpha[op])) + Vol(SV_\beta([a,b]))$. This indeed is the volume since the area enclosed by ac, cq and qa is equal in size to the area enclosed by fd, $d\bar{q}$ and $\bar{q}f$ where $\bar{q}$ is the point to where q would be swept when swept over angle α (and analogon for a,b,p).

For small angles we can compute the volume by:
$Vol(SV_\beta([ab])) + (Vol(SV_\alpha([oc])) - Vol(SV_\alpha([ob])))$.

case 3: Denote q for the intersection point of line oa and circle segment cf. Then the volume is $Vol(SV_\alpha([a,q])) + Vol(SV_\beta([a,b]))$. Again we use the similar property that the area between a, c, and q is equal to the area between d, f, and $\hat{q}$ where $\hat{q}$ is the point to which q would be swept when swept over angle α.

case 4: The volume now can be computed by $Vol(SV_\alpha([a,s])) + Vol(SV_\beta([a,c]))$ (similar to case 3).

6.3 Volume of Swept Volumes for Third and Fourth Link in the 4 DOF Case.

We can use the same technique here as in the previous subsection. In the following we will describe the volume computation for the fourth link. For the volume computation for the third link we just have to drop the accent ($'$) in the text.

case 1: Splitting up the volume to be computed in three now, we get similar to the 2 DOF case the volumes $Vol(CS_\beta([a,b']))$ and $Vol(\Delta ab'o) - Vol(SV_{\gamma'}([o,b'])$, where γ' is the angle between oa and ob', and the additional volume $Vol(\Diamond c'\tilde{c}'ha)$. The area of that parallelogram is equal to $l_e(m+m_e)\sin\xi$, since the sharp angle of the parallelogram is equal to ξ.

For small angles we compute: $Vol(SV_\beta([ab])) + Vol(\Delta abo) - (Vol(SV_\alpha([ob])) + Vol(\Delta oep))$ $+ Vol(\Diamond ac\tilde{c}\tilde{a})$. Again the area of the parallelogram is equal to $l_e(m+m_e)\sin\xi$.

case 2: The volume of the swept volume can now be computed by ($Vol(SV_\alpha([o,q]))$ - $Vol(SV_\alpha([o,p])))$ $+ Vol(SV_\beta([a,b'])) + Vol(\Diamond(a,g',\tilde{g}',\tilde{a}))$ where p is the intersection point of oa and be, q the intersection point of oa and $\tilde{c}'\bar{\tilde{c}}'$. The volume of the rectangle $\Diamond(a,g',\tilde{g}',\tilde{a})$ is exactly $l_e(m+m_e)$.

For small angles we compute the volume as follows: $Vol(SV_\alpha([oq])) - Vol(SV_\alpha([ob']) + Vol(SV_\beta([ab'])) + Vol(\Diamond g\tilde{g}'\tilde{a}'a) - (Vol(\Delta epo) - Vol(SV_\gamma([oe])))$, where q is the intersection of the line oa and circle segment $c'f'$, p is the intersection of the lines de and oa, and γ is the angle between the lines oa and oe.

case 3: Apart from the volume $Vol(SV_\alpha([oq]))$ - $Vol(SV_\alpha([oa]))$, where q is the intesection point of oa and $\tilde{c}'\bar{\tilde{c}}'$, we have to add $Vol(SV_\beta([a,b']))$ and $Vol(\Diamond(\tilde{c}', \tilde{b}', c', b'))$.

case 4: Apart from the volume $Vol(SV_\alpha([o\hat{s}]))$ - $Vol(SV_\alpha([oa]))$, where $\hat{s}$ is the intesection point of oa and $\tilde{c}'\tilde{b}'$, we have to add $Vol(SV_\beta([a,b']))$ and $Vol(\Diamond(\tilde{c}', \tilde{b}', c', b'))$.

In cases 3 and 4, we still have to compute the area of a parallelogram. All three of them have a basis of length l_e. The computation of the height can be done in the same way for both of them, as we will discribe now. The length of one of the edges of the parallelogram clearly is l_e. The other edge has length $2(m + m_e)\sin(\frac{\beta}{2})$, since the $\Delta a, b', c'$ is an isosceles triangle. The sharp angle ϵ of the parallelogram is $\zeta - (\frac{\pi-\beta}{2})$ and thus the area of the parallelogram is equal to $2l_e(m + m_e)\sin(\frac{\beta}{2})\sin\epsilon$.

7 Assuming Some Thickness for the Links: Line Extended to Rectangle.

In the previous we modelled the links by straight lines. In this section we model the links by rectangles. For the different shapes no major changes have to be made. The volume computation gets slightly more involved.

7.1 Extreme Points for Enclosure.

Let us introduce some new notations for the vertices of the rectangle. We thicken the line segment modelling a link to a rectangle. Each end of the line segment will now become the midpoint of the shorter edge of the rectangle. We will denote the vertices as depictured in Figure 5. The angle between ab'_1 and ab'_2 will be denoted by $\hat{\beta}$.

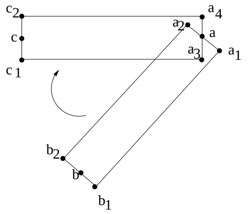

Figure 5: Notation.

The four cases we had before give rise to the following extensions considering a thickening of the line segment. Note however that in this situation Case 3 ends when the angle between oa and ab'_2, i.e. angle $\xi + \hat{\beta}$, is larger than π.

case 1: We now take for the extreme points the points $b_1, e_1, d_1, \tilde{d_1}, \tilde{d}, \tilde{d_4}, p_1, \tilde{a_4}, \tilde{c_2}, c_2, p_2$, where p_1 and p_2 are the intersection points of the tangents to the circle segments between the two points $\tilde{d_4}$ and $\tilde{a_4}$, respectively c_2 and b_1.

case 2: We take for extreme points $b_1, p, e_1, d_1, u, v, \tilde{d_4}, \tilde{f_2}, p_1, \tilde{c_2}, p_2, \tilde{g}, g, p_3$ if their polygon is convex, where p is the intersection point of oa with circle segment between b_1 and e_1. In the non-convex case and for small angles for α (for which oa does not intersect the circle segment between b_1 and e_1), we take for extreme points $b_1, e_1, d_1, u, v, \tilde{d_4}, \tilde{f_2}, p_1, \tilde{c_2}, p_2, \tilde{g}, g, p_3$. The points p_1,p_2,and p_3 are the intersection points of the tangents to the circle segments between the two points $\tilde{f_2}$ and $\tilde{c_2}$, $\tilde{c_2}$ and $\tilde{g}$, respectively g and b_1. Depending on the angle for β, u is $\tilde{d_1}$ and v is the intersection point of lines $\tilde{d_1}\tilde{d}$ and $d_4\tilde{d_4}$ for small β, or u is the intersection point of lines $d_1\tilde{d_1}$ and dd_4 and v is d_4 for small β. Here a large value for β means that $\beta > \pi - 2\zeta$, and small value for β means that $\beta < \pi - 2\zeta$. (When equality holds, d_1, $\tilde{d_1}$, d_4, and $\tilde{d_4}$ are collinear, in which case we can just forget about u and v.) Indeed, if and only if $\beta + 2\zeta > \pi$, the distance of d_1 to line od is smaller than the distance of d_4 to line od, and thus the line $d_1\tilde{d_1}$ will intersect dd_4.

case 3: Here we take $a_1, d_1, d, d_4, \tilde{d_4}, \tilde{f_2}, p_1, \tilde{c_2}, p_2, \tilde{b_1}, b_1$ where p_1 and p_2 are the intersection points of the tangents to the circle segments between the two points $\tilde{f_2}$ and $\tilde{c_2}$, respectively $\tilde{c_2}$ and $\tilde{b_1}$.

case 4: And in this case we take $a_4, a, a_1, b_1, \tilde{b_1}, p_1, \tilde{s}, p_2, \tilde{t}, p_3, \tilde{f_2}, f_2, d_4$, where p_1,p_2,and p_3 are the intersection points of the tangents to the circle segments between the two points $\tilde{b_1}$ and $\tilde{s}$, $\tilde{s}$ and $\tilde{t}$, and $\tilde{t}$ and $\tilde{f_2}$ respectively at these points. The points s_1 and s_2 are the vertices of the rectangle on the short edge of which s is the midpoint (i.e. after some rotation, point b was moved to s). Similarly points t_1 and t_2 correspond to t.

7.2 Volume Computation.

We can compute the volume swept by the rectangle in a similar way as in the case of a line. The main observation is that we now will consider the volumes swept by line segment ab_2, instead of by the line segment ab. On the appropriate places we then only have to add the area of the rectangle itself to the volumes computed for the line segment.

8 A 3D Case: Rectangle Extended to Cylinder.

We now extend the model of the links to cylinders. To the rectangles in the previous section we now add a height.

8.1 Extreme Points for Enclosure.

We will use the algorithm for enclosure of polygons by superellipsoids described in [Stifter 91]. For this algorithm we need a set of extreme points of a polygon.

We consider a Z-axis perpendicular to the plane in which the rectangle lies. We keep to all extreme points we already used in the previous section for the swept volume of the rectangle (we consider them now as points in 3 dimensional space with zero Z-coordinate). In each case we now add some points with non-zero Z-coordinate. These new points lie above and under (considered in the Z-direction) some points in the plane. For each such a point u in the plane we construct two new points u_+ and u_- with the same X- and Y-coordinates as u and with Z-coordinate h and $-h$ respectively, where h is the radius of the cylinder. The points we take for u are given in the following for each of the four cases.

case 1: $\tilde{a}, \tilde{d}, c, \tilde{c}, b, e, d$.

case 2: $b, e, d, \tilde{d}, \tilde{f}, \tilde{c}, g, \tilde{g}$.

case 3: $a, d, \tilde{d}, \tilde{f}, \tilde{c}, \tilde{b}, b$.

case 4: $a, d, f, \tilde{f}, \tilde{b}, b, \tilde{t}, \tilde{s}$.

8.2 Volume Computation.

We now have to compare the volume of the swept volume of a link with the volume of the enclosing superellipsoid. The volume of a superellipsoid can be approximated as described in [Zarrugh 85].

For the volume of the swept volume of the link modelled by a cylinder, we proceed as follows. Observe that the volume of the swept rectangle times the height of the cylinder is equal to the volume of a swept rectangular solid. This volume minus the difference in volume of the rectangular solid and the cylinder is the volume wanted. The volume of a rectangular solid and of a cylinder is trivial to compute, the volume of the swept rectangle in two dimensional space is done above.

8.2.1 First and Second Link.

We can compute the volume of the swept volume by adding $Vol(SV_{\alpha+\hat{\alpha}}([a, b'_2]))$, $Vol(\Delta ab'_2a_2)$, and $Vol(\Delta ab'_1a_2)$. Here $\hat{\alpha}$ stands for the angle between ab'_1 and ab'_2. The areas of the two triangles are the same and equal to $\frac{1}{2}h(l + l_e)\cos(\frac{\hat{\alpha}}{2})$.

8.2.2 Third and Fourth Link.

case 1: We add to the volume of the swept volume of line segment ab'_2, which can be computed as in the case of a robot arm modelled by line segments, the following areas: $Vol(\Diamond a_1b_1b_2a_2)$, $Vol(\Diamond \tilde{d}\tilde{d}_1d_1d)$, and the differences $Vol(SV_\alpha(oq)) - Vol(SV_\alpha(o\tilde{a}))$ and $Vol(SV_\alpha(op_1)) - Vol(SV_\alpha(op_2))$. Here q is the intersection point of line oa and circle segment $\tilde{a}_4\tilde{d}_4$, $p_1 = b_1e_1 \cap o\tilde{a}$, and $p_2 = b_2e_2 \cap o\tilde{a}$. Notice that the distance from o to p_1 is the same as the distance from o to b_1, and that the distance from o to p_2 is the same as the distance from o to c_1, which simplifies the computations.

In case angle α is small, q, p_1 or p_2 may not be in the swept volume. However, the computations can be done in the same way here, since we do not have to use these points in the computations themselves.

case 2: Here the volume can be computed by adding to the swept volume of line segment ab_2' the volumes: $Vol(\diamondsuit a_1 b_1 b_2 a_2)$, $Vol(\diamondsuit uv)$, and $(Vol(SV_\alpha([op_2]) - Vol(SV_\alpha([op_1])))$. Here $p_1 = oa \cap b_1 e_1$, and $p_2 = oa \cap b_2 e_2$. With $Vol(\diamondsuit uv)$ we mean a parallelogram with u and v as some of the vertices. There are two cases. If $u = \tilde{d_1}$ and $v = d_1\tilde{d} \cap d_4\tilde{d}_4$, then we have to compute the area of the parallelogram $d_1 u v \tilde{v}$. This area is equal to $(l + l_e)y_1$, where $y_1 = h(\sin(\frac{\pi}{2} - \zeta) - \sin(\xi + \beta - \frac{\pi}{2}))$. In case $u = d_1\tilde{d}_1 \cap dd_4$ and $v = d_4$, we have to compute the area of parallelogram $v\tilde{d}_4 u\tilde{u}$ which is equal to $(l + l_e)y_2$, where $y_2 = h(\sin(\xi + \beta - \frac{\pi}{2}) - \sin(\frac{\pi}{2} - \zeta))(= -y_1)$. We illustrate the computation of y_2 in Figure 6.

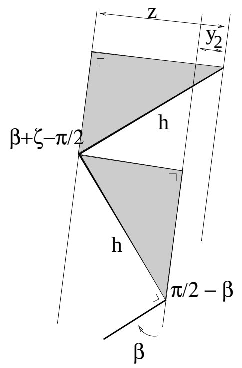

Figure 6: Computing y_2.

case 3: We add to the swept volume of line segment ab_1 the following areas: $Vol(\diamondsuit a_1 b_1 b_2 a_2)$, and the differences $Vol(SV_\alpha(oa)) - Vol(SV_\alpha(oa_1))$ and $Vol(SV_\alpha(o\tilde{c}_2)) - Vol(SV_\alpha(o\tilde{c}_1))$.

case 4: We add to the volume swept by line segment ab_2 the following areas: $Vol(SV_{\beta+\hat{\beta}}([a, b_1]) - Vol(\Delta ab_1 b_2)$, $Vol(\diamondsuit b_1 b_2 \tilde{b}_2 \tilde{b}_1)$, $Vol(\Delta a_1 a b_1)$, $Vol(\Delta f_2 d_4 d)$, and the volume swept by the line segments $a_1 a$ and aa_4 when swept over α.

For this last area there are two cases. If circle segment $a_1 d_1$ intersects aa_4, then we compute the intersection point (we denote it by r), and then add volumes $Vol(SV_\alpha(oa)) - Vol(SV_\alpha(oa_4))$, and $Vol(\Delta a_1 ar) - (Vol(SV_\gamma(oa)) - Vol(\Delta a_1 or))$, where γ is the angle between oa and or. In the other case, $d_1 d$ intersects circle segment $a_4 d_4$ and we can proceed in a similar way.

9 Counting It Out.

In this section we will compute and compare the volumes for some of the cases we have discussed. For this we have to consider a coordinate frame. In the two dimensional case we will take the first rotational joint (point o) as the origin of the frame, (the symmetry axis of) the first link oa

as Y-axis and the X-axis perpendicular to it. In the following we will denote the coordinates for point p by (px, py).

9.1 2 DOF's, case 1.

Straigthforward computations result in the following formulas for the coordinates of the extreme points.

p	px	py
a	0	l
b	$-m\sin\zeta$	$l - m\cos\zeta$
c	$-m\sin(\zeta+\beta)$	$l - m\cos(\zeta+\beta)$
d	$l\sin\alpha$	$l\cos\alpha$
e	$-l\sin\alpha - m\sin(\zeta-\alpha)$	$l\cos\alpha - m\cos(\zeta-\alpha)$
q	$\frac{m+\frac{\cos(\zeta+\beta)(\sin\zeta-\sin(\zeta+\beta))}{sin\beta}}{\sin(\zeta+\beta)}$	$l + \frac{m(\sin\zeta-\sin(\zeta+\beta))}{\sin\beta}$
r	$\frac{l}{\tan\alpha}(\sin\alpha+\cos\alpha-1)$	l

The centroid M of these 7 points can now be computed: Mx is the sum of the x-coordinates of the extreme points divided by 7, My is the sum of the y-coordinates of the extreme points divided by 7.

The main axis of the superellips, through M and parallel to ad, is given by the equation:

$$(\cos\alpha - 1)x - \sin\alpha y + yM\sin\alpha - (\cos\alpha - 1)xM = 0.$$

This allows us to compute the distance of a point to the main axis. When we do so for the extreme points, B will be defined as the largest distance among these increased by the tolerance ϵ.

For A, we proceed in the same way as for B but this time we compute the distance to the other axis of the superellips, namely:

$$\sin\alpha x + (\cos\alpha - 1)y - xM\sin\alpha + (\cos\alpha - 1)yM = 0.$$

9.2 2 DOF's, case 2.

In this case we can have two different sets of extreme points. The coordinates of all these points can be computed in a straightforward way. The table below summarizes the results.

p	px	py
b	$-m\sin\zeta$	$l-m\cos\zeta$
c	$-m\sin(\zeta+\beta)$	$l-m\cos(\zeta+\beta)$
d	$l\sin\alpha$	$l\cos\alpha$
e	$-l\sin\alpha-m\sin(\zeta-\alpha)$	$l\cos\alpha-m\cos(\zeta-\alpha)$
f	$-l\sin\alpha-m\sin(\xi-\alpha)$	$l\cos\alpha-m\cos(\xi-\alpha)$
p	0	$\sqrt{l^2+m^2-2lm\cos\zeta}$
s	$\frac{(l^2+m^2-2lm\cos(\zeta+\beta))(yc-yf)}{xf.yc-xc.yf}$	$\frac{(l^2+m^2-2lm\cos(\zeta+\beta))(xf-xc)}{xf.yc-xc.yf}$
t	$xa+\frac{m^2(yc-yb)}{(yc-ya)(xb-xa)-(yb-ya)(xc-xa)}$	$ya+\frac{m^2(xb-xc)}{(yc-ya)(xb-xa)-(yb-ya)(xc-xa)}$

The coordinates of point p are obtained by considering the triangle aob, and those of points s and t by intersecting the appropriate tangent lines to a sphere. For point s we also considered the triangle aoc. For the centroid of these points and for the first axis (and thus for the determination of A and B) we proceed as in case 1.

9.3 2 DOF's, case 3.

We have for the coordinates of the extreme points in this case the following table.

p	px	py
a	0	l
b	$-m\sin\zeta$	$l-m\cos\zeta$
c	$-m\sin(\zeta+\beta)$	$l-m\cos(\zeta+\beta)$
d	$l\sin\alpha$	$l\cos\alpha$
f	$-l\sin\alpha-m\sin(\xi-\alpha)$	$l\cos\alpha-m\cos(\xi-\alpha)$
p	$xa+\frac{m^2(yc-yb)}{(xb-xa)(yc-ya)-(xc-xa)(yb-ya)}$	$ya+\frac{m^2(xb-xc)}{(xb-xa)(yc-ya)-(xc-xa)(yb-ya)}$
q	$\frac{(l^2+m^2-2lm\cos(\zeta+\beta))(yc-yf)}{xf.yc-xc.yf}$	$\frac{(l^2+m^2-2lm\cos(\zeta+\beta))(xf-xc)}{xf.yc-xc.yf}$

For the centroid of these points and for the first axis (and thus for the determination of A and B) we proceed as in case 1.

9.4 2 DOF's, case 4.

Finally in the fourth case we have the following coordinates for the extreme points.

p	px	py
a	0	l
b	$-m\sin\zeta$	$l-m\cos\zeta$
d	$l\sin\alpha$	$l\cos\alpha$
f	$-l\sin\alpha-m\sin(\xi-\alpha)$	$l\cos\alpha-m\cos(\xi-\alpha)$
s	0	$l+m$
t	$-(l+m)\sin\alpha$	$(l+m)\cos\alpha$

For the centroid of these points and for the first axis (and thus for the determination of A and B) we proceed as in case 1.

9.5 The Exponent.

Finally we come to the determination of the exponent. We can use the approach in [Stifter 91] where the exponent is adapted until all points are inside the superellips. However, we can compute for all extreme points a safe approximation of the exponent for which that particular point is inside a superellips with given A and B and then choose the biggest one of those computed exponents (so that all points are inside). For this we have to solve the equation of the superellips to exponent n. We can approximate the solution by computing the Taylor series. Note that without loss of generality we can assume that the extreme points all lie in the first quadrant (if for point p this is not the case, we take the point $(|px|, |py|)$ instead). Also without loss of generality we can assume that A and B are 1, by adapting the coordinates of the extreme points. We let Computer Algebra Systems compute the Taylor series for the equation $x^m + y^m - 1$ around point $(\frac{1}{2}, \frac{1}{2})$ so that we have an expression for$m$ in function of x and y. This value then can be used as an initial guess for the exponent, and can be adapted as in [Stifter 91].

If we want to be sure that the resulting exponent is a safe one, we also have to look at the error estimate for the Taylor expansion. Also for checking its convergence we need the error estimate. Currently we did not succeed in computing the error term for the equation we considered with any of the Computer Algebra Systems with which we tried. For this we have to consider the result of the Taylor series as an initial guess rather than a safe approximation for the exponent.

10 Conclusions.

For our purposes we need a good approximation of swept volumes of robot arm links. We enclose them by superellipses or superellipsoids, in order to be able to use the Roider Method for superellipses and superellipsoids.

Here we have demonstrated that it is possible to model these swept areas using some elementary geometrical and trigonometrical tools. We have described for all swept volumes occuring for some robot arm topologies the extreme points needed for the enclosure of solids by a superellips or by a superellipsoid. We also computed the volume of the swept areas and of the enclosing superellips or superellipsoid. The rate between these volumes is a measure for the accuracy of the enclosure.

References

[Barr 81] **Barr, A. H.** , Superquadrics and Angle-Preserving Transformations, IEEE Computer Graphics and Applications, Vol. III, January 1981, pp. 11-23.

[Dittenberger 87] **Dittenberger, K.** , How to Enclose Boxes, Cylinders, Cones, and Pyramids Using Superellipsoids, Technical Report, RISC-Linz, 87-34.1.

[Stifter 88b] **Stifter, S.** , An Algorithm to Enclose Objects in a Robot Working Cell by Superellipsoids, Technical Report, RISC-Linz, 88-72.0.

[Stifter 88c] **Stifter, S.** , A Generalisation of the Roider Method to Solve the Robot Collision Problem in 3D, In Proceedings of International Symposium on Symbolic and Algebraic Computation (ISSAC '89), Rome, Italy, July 4-8, Springer LNCS 358, pp. 332-343, 1988.

[Stifter 91] **Stifter, S.** , Collision Detection in the Robot Simulation System SMART, International Journal of Advanced Manufacturing Technology, Vol. 7, 1992, pp. 277-284.

[Van Geem 94] **Van Geem, C.** , On Using a Manhattan Distance-like Function for Robot Motion Planning on a Non-Uniform Grid in Configuration Space, Technical Report, RISC-Linz, 94-74, To appear in the Austrian Issue of the International Journal Flexible Automation and Integrated Manufacturing (FAIM).

[Zarrugh 85] **Zarrugh M. Y.** , Display and Inertia Parameters of Superellipsoids as Generalized Constructive Solid Geometry Primitives, In Proceedings of the 1985 ASME International Computers in Engineering Conference and Exhibition, August 4-8, 1985, Boston, MA, Vol. 1, pp. 317-328.